BIOCHEMISTRY
including biophysical chemistry & molecular biology

Article

pubs.acs.org/biochemistry

A Typical Preparation of *Francisella tularensis* *O*-Antigen Yields a Mixture of Three Types of Saccharides

Qi Wang,[†] Xiaofeng Shi,[†] Nancy Leymarie,[†] Guillermo Madico,[‡] Jacqueline Sharon,[‡] Catherine E. Costello,[†] and Joseph Zaia*[,†]

[†]Department of Biochemistry, Boston University School of Medicine, Boston, Massachusetts 02118, United States

[‡]Department of Pathology and Laboratory Medicine, Boston University School of Medicine, Boston, Massachusetts 02118, United States

Supporting Information

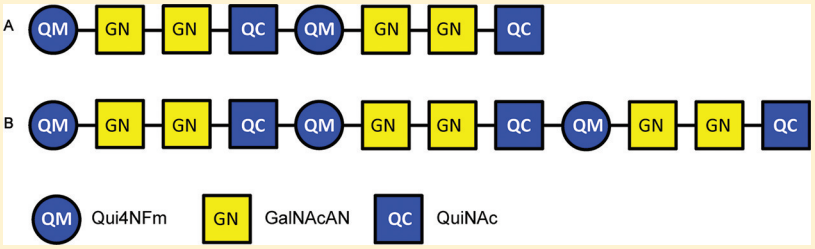

ABSTRACT: Tularemia is a severe infectious disease in humans caused by the Gram-negative bacterium *Francisella tularensis* (Ft). Because of its low infectious dose, high mortality rate, and the threat of its large-scale dissemination in weaponized form, development of vaccines and immunotherapeutics against Ft is essential. Ft lipopolysaccharide (LPS), which contains the linear graded-length saccharide component *O*-antigen (OAg) attached to a core oligosaccharide, has been reported as a protective antigen. Purification of LPS saccharides of defined length and composition is necessary to reveal the epitopes targeted by protective antibodies. In this study, we purified saccharides from LPS preparations from both the Ft subspecies *holarctica* live vaccine strain (LVS) and the virulent Ft subspecies *tularensis* SchuS4 strain using liquid chromatography. We then characterized the fractions using high-resolution mass spectrometry and tandem mass spectrometry. Three types of saccharides were observed in both the LVS and SchuS4 preparations: two consisting of OAg tetrasaccharide repeats attached to one of two core oligosaccharide variants and one consisting of tetrasaccharide repeats only (coreless). The coreless OAg oligosaccharides were shown to contain Qui4NFm (4,6-dideoxy-4-formamido-D-glucose) at the nonreducing end and QuiNAc (2-acetamido-2,6-dideoxy-*O*-D-glucose) at the reducing end. Purified homogeneous preparations of saccharides of each type will allow mapping of protective epitopes in Ft LPS.

Francisella tularensis (Ft) is the Gram-negative bacterium that causes tularemia, an infectious disease in humans and other mammals, including aquatic rodents and rabbits. Ft is classified as a category A Select Agent by the Centers for Disease Control because of its low infectious dose and high mortality rate. The infectious dose for respiratory tularemia is <10 colony forming units,[1] with a mortality rate of 5−30% for untreated disease.[2] Tularemia is normally treated with antibiotics, but the mortality rate is still 2−3% in treated patients.[3−5] A strain of type B (subspecies *holarctica*) Ft, live vaccine strain (LVS), was developed in the former Soviet Union in 1961.[6] To date, this is the only vaccine that has partial protective effects in humans against the most virulent type A (subspecies *tularensis*) Ft strains that include SchuS4.[7,8] LVS is not approved by the U.S. Food and Drug Administration as a vaccine for the general public because of safety concerns.[9,10] Therefore, development of new vaccines and immunotherapeutics for tularemia is essential.

Lipopolysaccharide (LPS) has been reported as a protective Ft antigen, with antibodies targeting primarily its saccharide components.[11−14] LPS is comprised of three parts: lipid A, core oligosaccharides, and *O*-antigen (OAg). Lipid A is anchored in the outer membrane of Ft, and the core and OAg extend from the bacterial surface.[15] OAg is a linear saccharide comprised of tetrasaccharide repeats, normally attached to the nonreducing end mannose residue of the core oligosaccharide. The structure of Ft LPS has been studied using nuclear magnetic resonance (NMR) and mass spectrometry (MS), as reviewed in ref 15. In 1991, Vinogradov and co-workers reported the first Ft OAg structure, determined using NMR for type B Ft strain 15.[16] The OAg was identified as containing a variable number of tetrasaccharide $GalNAcAN_2QuiNAcQui4NFm$ repeats, i.e., 2 mol of 2-acetamido-2-deoxy-*O*-D-galacturonamide (GalNAcAN), 1 mol of 2-acetamido-2,6-dideoxy-*O*-D-glucose (QuiNAc), and 1 mol of 4,6-dideoxy-4-formamido-D-glucose (Qui4NFm).[16] In their later study, the lipid A and core

Received: September 17, 2011
Revised: November 16, 2011
Published: November 17, 2011

oligosaccharide structures were also determined.[17] There are two types of core structures: $HexNAcHex_3Kdo$, i.e., one with 1 mol of *N*-acetylhexosamine (HexNAc), 3 mol of hexoses (Hex), and 1 mol of 3-deoxy-D-*manno*-oct-2-ulosonic acid (Kdo), and $HexNAcHex_4Kdo$. The structures of OAg and core oligosaccharides in type A Ft were identical to those observed in type B Ft.[18,19] In a recent report, a Ft capsular polysaccharide (CPS) was shown to consist of the same GalNAcAN$_2$QuiNAcQui4NFm tetrasaccharide repeat as OAg and to protect mice against LVS Ft challenge.[20]

To develop vaccines and immunotherapeutics against Ft, it is necessary to determine the saccharide structure(s) recognized by protective antibodies. Toward this end, the compositions and linkages of saccharides from LPS preparations of both the LVS and SchuS4 strains were analyzed using liquid chromatography (LC), high-resolution mass spectrometry, and tandem mass spectrometry (MS^n). Contrary to earlier studies in which low-resolution mass spectrometry was used and MS/MS was not employed,[18] three types of saccharides were observed in LPS preparations of both strains: two consisting of OAg attached to one of two core oligosaccharide variants and one consisting of OAg only. Because all three have the potential to generate an immune response toward Ft, these results represent significant new information that impacts the development of immunotherapeutics based on protective antibodies.

MATERIALS AND METHODS

LPS Preparations. LPS from Ft LVS was purchased from Sussex Research (Ottawa, ON). LPS from Ft SchuS4 was prepared as follows. SchuS4 bacteria (NR-643, obtained from BEI Resources, Manassas, VA) were grown to confluence on chocolate agar plates (Remel, Lenexa, KS) for 3 days at 35 °C. Bacteria were scraped and suspended in phosphate-buffered saline, heat-killed at 82 °C for 2 h, and supplemented with sodium azide to a final concentration of 0.1%. Bacteria originating from 20 plates, with a total OD_{600} of 343, were used for LPS purification by a hot phenol/water extraction method[21,22] with modifications. Briefly, the cell suspension was lyophilized and reconstituted with 25 mL of high-performance liquid chromatography-grade water, and the resulting suspension was heated to 68 °C. An equal volume of a 90% phenol solution, preheated to 68 °C, was added, and the mixture was incubated at 68 °C for 1 h with vigorous stirring. After being kept for 1 h on ice, the mixture was centrifuged at 3300*g* for 10 min at 4 °C, and the aqueous phase was aspirated. After 25 mL of water that had been heated to 68 °C was added to the organic phase, the mixture was incubated at 68 °C for 1 h, with vigorous stirring. After 1 h on ice, the mixture was centrifuged at 3300*g* for 10 min at 4 °C. The aqueous phase was aspirated and combined with the previous fraction. The combined aqueous solution was dialyzed extensively versus water and then concentrated using rotary evaporation at 40 °C. The residual solution was lyophilized overnight. The lyophilized powder was reconstituted with 10 mL of 0.3 M sodium acetate and 70 mL of ice-cold absolute ethanol. After being cooled in a freezer at −80 °C, the solution was incubated at −20 °C for 2 h and centrifuged at 10000*g* for 20 min at 4 °C, and the pellet was reconstituted with 10 mL of water and 70 mL of ice-cold absolute ethanol. A pellet was obtained by centrifugation at 10000*g* for 20 min at 4 °C and resuspended in 1 mL of 50 mM Tris-HCl (pH 8.0) with 2 mM $MgCl_2$. Benzonase (600 milliunits) was added, and the sample was incubated at 37 °C for 3 h. After inactivating the enzyme by heating the mixture at 99 °C for 5 min, we adjusted the buffer to 1 mM $CaCl_2$. Pronase (1 mg) was added, and the sample was incubated at 55 °C for 24 h. After overnight lyophilization, 20 mg of material was obtained.

Release and Derivatization of Saccharides Purified from LPS. Saccharides were released from LPS by incubation in 1% acetic acid at 100 °C for 2.5 h, and the resulting oligosaccharides were separated from lipid A by aspiration of the supernatant after centrifugation at 11000*g* for 1 h. Reduction and permethylation were performed using published procedures.[18,23,24]

Size Exclusion Chromatography (SEC). Saccharides from SchuS4 and LVS LPS were fractionated using SEC (Superdex Peptide 10/300 GL, GE Healthcare) using a 100 mM ammonium acetate/10% acetonitrile mixture as the mobile phase. The flow rate was 0.2 mL/min with a 2 h isocratic gradient, and UV detection at 225 nm was used for monitoring sample elution. An automatic fraction collector was used with an interval of 2 min per eluted fraction.

Mass Spectrometry and Data Analysis. *Matrix-Assisted Laser Desorption Ionization Time-of-Flight (MALDI-TOF) MS.* A Reflex IV MALDI-TOF mass spectrometer (Bruker Daltonics, Billerica, MA) equipped with a nitrogen laser (337 nm, 3 ns pulse width) was used. The matrix solution consisted of 10 mg/mL 2,5-dihydroxybenzoic acid (DHB) in a 0.1% trifluoroacetic acid (TFA)/10 μM sodium bicarbonate/50% acetonitrile mixture. The saccharide samples (0.5 μL) were allowed to cocrystallize with 0.5 μL of matrix solution on a stainless steel target. Signals from 400 laser shots at 25−40% laser power were accumulated in positive ion mode over the range of m/z 500−8000. To optimize detection of high-molecular weight saccharides in the derivatized sample, the detection range was set to m/z 2500−8000. External calibration was achieved using peptide calibration standard II (Bruker Daltonics). DataAnalysis 4.0 (Bruker Daltonics) was used for data analysis.

Chip-Based Liquid Chromatography and Mass Spectrometry. Saccharides from LVS and SchuS4 strains without SEC fractionation were analyzed by hydrophilic interaction chromatography (HILIC) and MS using a makeup flow (MUF)-chip-based mass spectrometer interface (Agilent Technologies, Santa Clara, CA) and a published procedure.[25] Formic acid (50 mM, pH 4.4) with ammonia containing 10% acetonitrile was used as mobile phase A. Mobile phase B consisted of 95% acetonitrile and 5% mobile phase A. A gradient composed of 90% B was used to load oligosaccharide samples on the enrichment column at a flow rate of 4 μL/min for a 30 μL volume. A gradient from 90 to 0% B was delivered over 39 min using a nanoflow pump at a rate of 200 nL/min. Pure acetonitrile was used as the MUF at 200 nL/min. An Agilent 6520 quadrupole TOF mass spectrometer was used for detection in negative ionization mode.

High-Resolution and High-Accuracy Mass Spectrometric Analysis. SEC-fractionated SchuS4 OAg saccharides were analyzed with an LTQ-Orbitrap XL instrument (ThermoFisher Scientific, San Jose, CA) and a hybrid qQh FT-ICR mass spectrometer (SolariX 12T, Bruker Daltonics) to achieve high-resolution and high-accuracy measurements. The samples were diluted in 50% methanol for negative ion mode detection and in a 20 μM sodium bicarbonate/50% acetonitrile mixture for positive ion mode detection. The FT-ICR mass spectrometer was calibrated with ESI tuning mix (part number G2432A,

Agilent Technologies). The capillary voltage was set to 1200 V, and nitrogen was used as the drying gas at a flow rate of 2.5 L/min. The mass spectra were recorded over the range of m/z 400−3000. The collision voltage was set to 5 V for fragmentation of [4,2,2][0,0,0] and 10 V for [6,3,3][0,0,0], and argon was used as the collision gas. DataAnalysis 4.0 (Bruker Daltonics) was used for data analysis.

The LTQ-Orbitrap XL instrument is equipped with a NanoMate TriVersa ion source (Advion, Ithaca, NY). The capillary voltage was set to 1.5 kV, and the gas pressure was set to 0.4 psi. The mass spectra were recorded over the range of m/z 200−2000 at a resolution of 100000. After external calibration, the mass accuracy remained within 5 ppm. The normalized collision energy for collision-induced dissociation (CID) was set to 20%, and helium was used as the collision gas. All spectra were recorded in profile mode. Xcalibur 2.0.7 (ThermoFisher Scientific) was used for data analysis.

RESULTS

MALDI-TOF MS of LVS LPS. To confirm published reports and establish separation conditions, we analyzed native saccharides derived from a commercial preparation of LVS LPS and their derivatives that had been subjected to reduction and permethylation using MALDI-TOF MS in positive ion mode. Peaks corresponding to the oligosaccharide compositions $HexNAcHex_3Kdo$ and $HexNAcHex_4Kdo$, which are the two types of core structures of LPS,[18] were observed in both the native and permethylated samples (Figure 1 and Table 1).

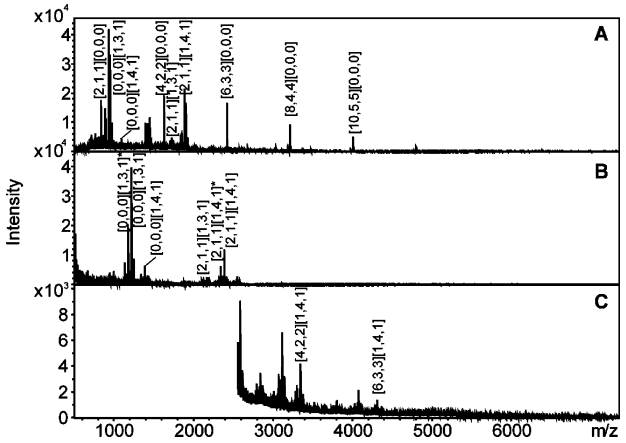

Figure 1. MALDI-TOF mass spectra of native (A) and reduced and permethylated LVS saccharide chains in the low-molecular weight (B) and high-molecular weight (C) ranges. Saccharide compositions are given as [GalNAcAN,QuiNAc,Qui4NFm][HexNAc,Hex,Kdo].

Glycans resulting from sequential addition of a tetrasaccharide unit consisting of $GalNAcAN_2QuiNAcQui4NFm$ to the $HexNAcHex_4Kdo$ core structure were also observed in both samples. However, peaks corresponding to the saccharides composed of one to nine tetrasaccharide repeats without an attached core, which had compositions identical to that of Ft CPS,[20] were observed only in the mass spectrum generated from the native sample. The mass spectra of the saccharides after permethylation (Figure 1B,C) are largely consistent with the previously published work of Prior et al,[18] and the observed ions correspond to OAg with the $HexNAcHex_4Kdo$ core. It is noteworthy that OAg attached to the $HexNAcHex_3Kdo$ core, [2,1,1][1,3,1] (the saccharide composition is given as [GalNAcAN,QuiNAc,Qui4NFm][HexNAc,Hex,Kdo]), has been detected in both the native and permethylated samples. These data represent the first time that [2,1,1][1,3,1] has been reported. The mass assignments for the MALDI-TOF MS results are listed in Table 1. The detection of native saccharides in the LPS preparation demonstrates that the material previously thought to consist only of OAg attached to the $HexNAcHex_4Kdo$ core is actually comprised of three types of chains: OAg attached to the $HexNAcHex_4Kdo$ core, OAg attached to the $HexNAcHex_3Kdo$ core, and OAg with no attached core (coreless saccharides).

Table 1. Observed Ions for Native and Reduced and Permethylated LVS Saccharides in Positive Ion Reflectron Mode on a MALDI-TOF Mass Spectrometer[a]

saccharide composition	observed m/z (native)	observed m/z (permethylated)
[2,1,1][0,0,0]	833.8	
[0,0,0][1,3,1][b]		1172.6
[0,0,0][1,3,1]	932.7	1218.6
[0,0,0][1,4,1]	1094.7	1421.2
[4,2,2][0,0,0]	1626.2	
[2,1,1][1,3,1]	1725.2	2179.2
[2,1,1][1,4,1][b]		2338.3
[2,1,1][1,4,1]	1887.3	2384.3
[4,2,2][1,4,1]		3345.8
[6,3,3][1,4,1]		4307.5
[6,3,3][0,0,0]	2419.8	
[8,4,4][0,0,0]	3212.3	
[10,5,5][0,0,0]	4005.7	

[a] Saccharide compositions are given as [GalNAcAN,QuiNAc,Qui4NFm][HexNAc,Hex,Kdo]. [b] Represents the loss of formic acid.

Relative Abundances of Saccharides from LVS and SchuS4 LPS Preparations. To determine whether the three types of saccharide chains observed in the LVS LPS preparation are also present in an LPS preparation derived from the virulent SchuS4 strain, we analyzed saccharides from SchuS4 LPS purified in house. The relative abundances of the saccharide chains in the LPS preparations from both the LVS and SchuS4 strains were determined using a chip-based LC−MS system. All saccharides found in LVS were also found in SchuS4, and both strains were found to have higher abundances of OAg core saccharides containing the $HexNAcHex_4Kdo$ core ([1,4,1]) than the corresponding saccharides containing the $HexNAcHex_3Kdo$ core ([1,3,1]) (Figure 2). Coreless saccharides $[2,1,1]_{1-9}[0,0,0]$ were found in considerably higher abundances in SchuS4 than in LVS. In the LVS preparation, the [0,0,0][1,3,1] core oligosaccharide was the most abundant component and the LVS saccharide [2,1,1][1,4,1] was also detected in high abundance. The results show dramatically different abundances of saccharides in the OAg fractions from the LVS and SchuS4 preparations, but these differences may not be explained solely by the differences between the strains because growth conditions can affect LPS saccharide composition in Ft.[26]

Tandem MS of LPS Coreless Saccharides. *[4,2,2]-[0,0,0].* Tandem MS was performed on the saccharides with two and three tetrasaccharide repeats. The oligosaccharide containing two tetrasaccharide repeats, [4,2,2][0,0,0], was enriched using SEC. The peak at m/z 824.2961 corresponds to the $[M + 2Na]^{2+}$ ion of [4,2,2][0,0,0] with a −1.1 ppm mass

dx.doi.org/10.1021/bi201450v | Biochemistry 2011, 50, 10941−10950

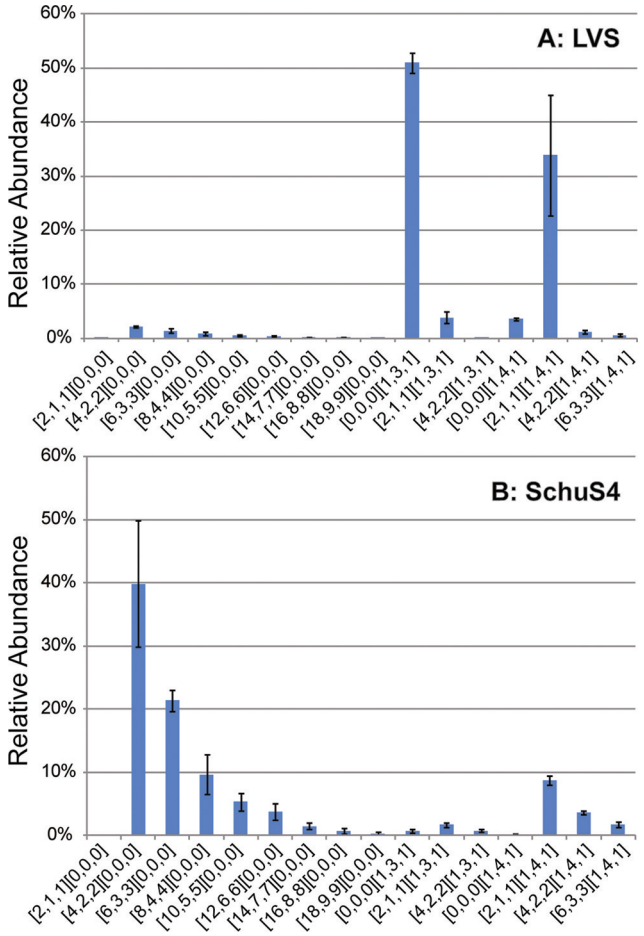

Figure 2. Relative abundances of saccharide chains in LPS preparations from LVS (A) and SchuS4 (B) Ft strains. The relative abundances were obtained from integration of the areas under the peaks in the extracted ion chromatograms for each compound from HILIC chip-based LC–MS. Error bars were calculated as standard deviations from the means of triplicate determinations. Saccharide compositions are given as [GalNAcAN,QuiNAc,Qui4NFm]-[HexNAc,Hex,Kdo].

error. This ion was subjected to tandem MS using CID in positive ion mode on an LTQ-Orbitrap XL mass spectrometer (Figure 1A of the Supporting Information). To further characterize the topology of this saccharide, the product ion at m/z 833.3009 from the MS^2 spectrum, which corresponds to the sodium-adducted fragment containing the tetrasaccharide [2,1,1][0,0,0], was isolated and subjected to further CID fragmentation. In the resulting MS^3 spectrum (Figure 1B of the Supporting Information), the two ions with the highest signal intensities corresponding to [2,0,1][0,0,0] and [2,1,0][0,0,0] were each isolated and fragmented with another stage of CID. The resulting MS^4 spectra for fragmentation of ions at m/z 646.2158 ([2,0,1][0,0,0]) and m/z 660.2314 ([2,1,0][0,0,0]) are shown in Figure 1C,D of the Supporting Information. The detailed interpretations of the multistage tandem MS results are listed in Table 1 of the Supporting Information. The fragment ions were reported using the Domon and Costello nomenclature.[27] Fragments corresponding to [2,0,0][0,0,0] and [1,0,1][0,0,0] were observed in the MS^4 spectrum of [2,0,1][0,0,0], and these indicate the Qui4NFm-GalNAcAN-GalNAcAN monosaccharide sequence. In the MS^4 spectrum of [2,1,0][0,0,0], the observation of [2,0,0][0,0,0] and [1,1,0]-[0,0,0] fragments suggests the GalNAcAN-GalNAcAN-QuiNAc monosaccharide sequence. The existence of [2,0,1][0,0,0] and [2,1,0][0,0,0] fragments in the MS^3 spectrum, together with the monosaccharide sequences deduced from the MS^4 spectra, shows that Qui4NFm-GalNAcAN-GalNAcAN-QuiNAc is the monosaccharide sequence of [2,1,1][0,0,0]. Analysis of the fragments in the MS^2 spectrum that resulted from glycosidic bond cleavages led to the conclusion that the precursor ion at m/z 824.2961, assigned to [4,2,2][0,0,0], is composed of two tetrasaccharide repeats, Qui4NFm-GalNAcAN-GalNAcAN-QuiNAc, in series.

Although the [4,2,2][0,0,0] monosaccharide sequence was assigned on the basis of MS^n analysis of the native glycan, tandem MS of the ^{18}O-labeled sample was necessary to unambiguously assign the residue at the reducing end (Figure 2 of the Supporting Information). The ions observed at m/z 825.2987 correspond in composition to $[M + 2Na]^{2+}$ for [4,2,2][0,0,0], with one ^{16}O being replaced by one ^{18}O with a −0.5 ppm mass error. After isolation of the ions in the quadrupole ion trap, CID resulted in the formation of the fragments at m/z 835.3053 in the MS^2 spectrum, which correspond to the sodium adduct of [2,1,1][0,0,0] with one ^{18}O atom replacing one ^{16}O atom (Figure 2A of the Supporting Information). After isolation of the peak at m/z 835.3053, MS^3 was performed (Figure 2B of the Supporting Information). The detailed interpretations of the multistage tandem MS results are listed in Table 2 of the Supporting Information. The two most abundant MS^3 product ions were observed at m/z 646.2163 and 662.2362 and were consistent with trisaccharide compositions of [2,0,1][0,0,0] and one ^{18}O atom replacing one ^{16}O atom of [2,1,0][0,0,0], respectively. From this result, a QuiNAc residue was determined to be located at the reducing end of [4,2,2][0,0,0]. The [4,2,2][0,0,0] glycan is therefore composed of two tetrasaccharide repeats, Qui4NFm-GalNAcAN-GalNAcAN-QuiNAc, in series, with a Qui4NFm residue at the nonreducing end and a QuiNAc residue at the reducing end (Figure 3A).

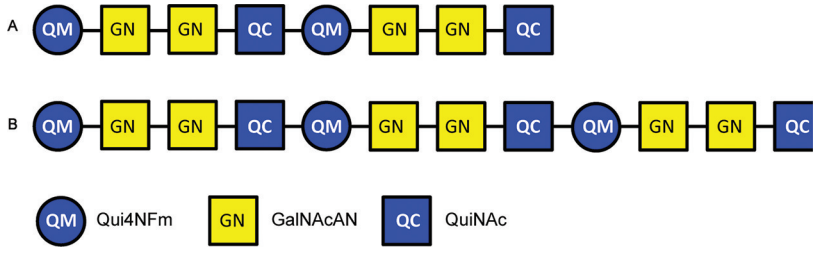

Figure 3. Structures of coreless saccharides [4,2,2][0,0,0] (A) and [6,3,3][0,0,0] (B) deduced from tandem MS in both positive and negative ion modes.

dx.doi.org/10.1021/bi201450v | *Biochemistry* 2011, 50, 10941–10950

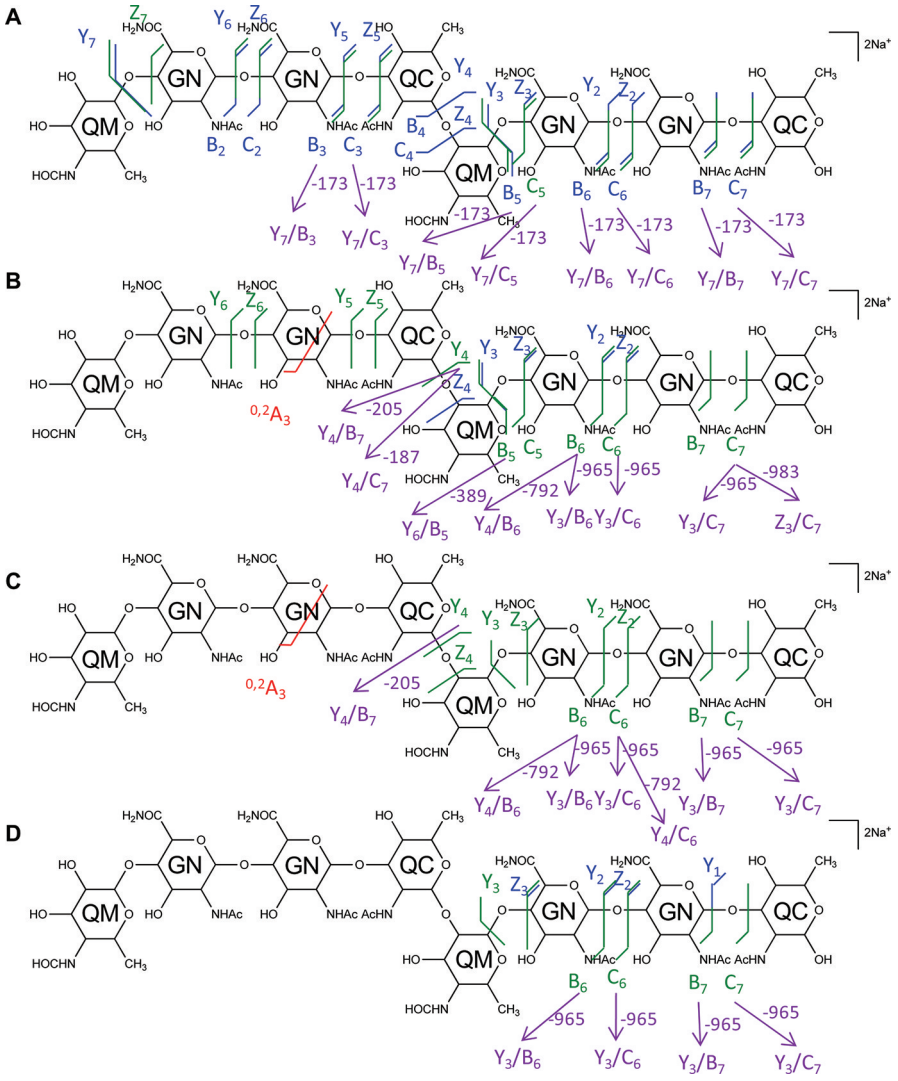

Figure 4. Multistage tandem MS reveals the structural linkage for [4,2,2][0,0,0]. Tandem MS of saccharide [4,2,2][0,0,0], $[M + 2Na]^{2+}$ ion at m/z 824.2961, and its product ions was performed on an LTQ-Oribtrap XL mass spectrometer in positive ion mode. CID fragmentations of the precursor ion at m/z 824.2961 (A), MS^3 of the ion at m/z 833.3009 (B), and MS^4 of the ions at m/z 646.2158 (C) and m/z 660.2314 (D) are displayed on the chemical structures with glycosidic bond cleavages labeled in blue, cross-ring cleavages in red, and internal cleavages in green. Monosaccharide residue abbreviations QM (Qui4NFm), GN (GalNAcAN), and QC (QuiNAc) are shown inside the six-member rings for the sake of clarity. One pair of internal cleavages is shown in purple to represent the alternative assignments. All fragments contain Na.

The multistage tandem MS fragments of native and ^{18}O-labeled [4,2,2][0,0,0] are displayed on their chemical structures in Figures 4 and 5, with glycosidic bond cleavages labeled in blue, internal cleavages in green, and cross-ring cleavages in red. Observed glycosidic bond cleavages provided monosaccharide sequence information, and the presence of the $^{0,2}A_3$ cleavage in panels B and C of Figure 4 verified the nonreducing end saccharide mass.

To confirm these results, we conducted tandem MS of native [4,2,2][0,0,0] in negative ion mode using a Fourier transform ion cyclotron resonance (FT-ICR) mass spectrometer (Figure 3A of the Supporting Information). The mass spectral data were more accurate than those acquired with the LTQ-Orbitrap XL mass spectrometer and thus provided the advantage of greater certainty of mass assignments. The detailed interpretations of the tandem MS result are presented in Figure 6A and Table 3 of the Supporting Information. Fragmentation patterns similar to those found in the negative ion MS/MS spectra were observed in the MS/MS spectra acquired in the positive ion mode using the LTQ-Orbitrap XL mass spectrometer. The observed glycosidic bond cleavages confirmed that [4,2,2]-[0,0,0] is composed of two tetrasaccharide repeats, Qui4NFm-GalNAcAN-GalNAcAN-QuiNAc, in series. Cross-ring cleavages were observed in higher abundances in negative ion mode using the FT-ICR mass spectrometer than in positive ion mode using the LTQ-Orbitrap mass spectrometer but did not allow unambiguous assignment of linkages.

[6,3,3][0,0,0]. The oligosaccharide corresponding to the coreless chain [6,3,3][0,0,0] was also analyzed using multistage tandem MS in positive ion mode on an LTQ-Orbitrap XL mass spectrometer. The $[M + 2Na]^{2+}$ peak at m/z 1220.4479 was isolated and subjected to CID (Figure 4A of the Supporting Information). The tetrasaccharide product ion observed at m/z 833.3003 in the MS^2 spectrum, which corresponds to [2,1,1][0,0,0], was isolated and fragmented using CID (Figure 4B of the Supporting Information). The detailed interpretations of the multistage tandem MS results are listed in Table 4 of the Supporting Information. As was the case for the MS^3 spectrum

dx.doi.org/10.1021/bi201450v | *Biochemistry* 2011, 50, 10941–10950

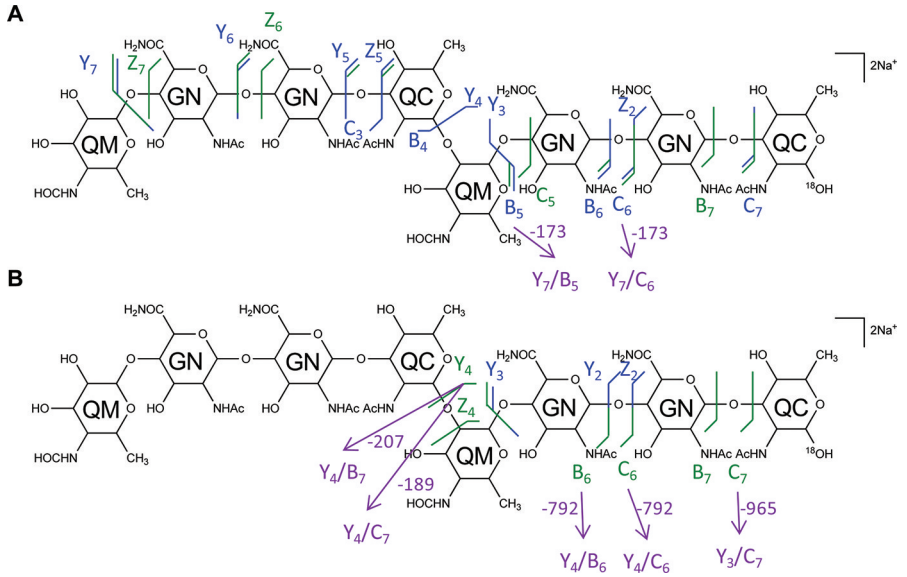

Figure 5. Multistage tandem mass spectra of ^{18}O-labeled saccharide [4,2,2][0,0,0] reveal the reducing end residue. Tandem MS of ^{18}O-labeled saccharide [4,2,2][0,0,0] was performed on an LTQ-Oribtrap XL mass spectrometer in positive ion mode. CID fragmentations of the precursor $[M + 2Na]^{2+}$ ion at m/z 825.2987 (A) and MS^3 of the secondary product ion at m/z 835.3053 (B) are displayed on the chemical structures. Monosaccharide residue abbreviations QM (Qui4NFm), GN (GalNAcAN), and QC (QuiNAc) are shown inside the six-member rings for the sake of clarity. All fragments contain Na.

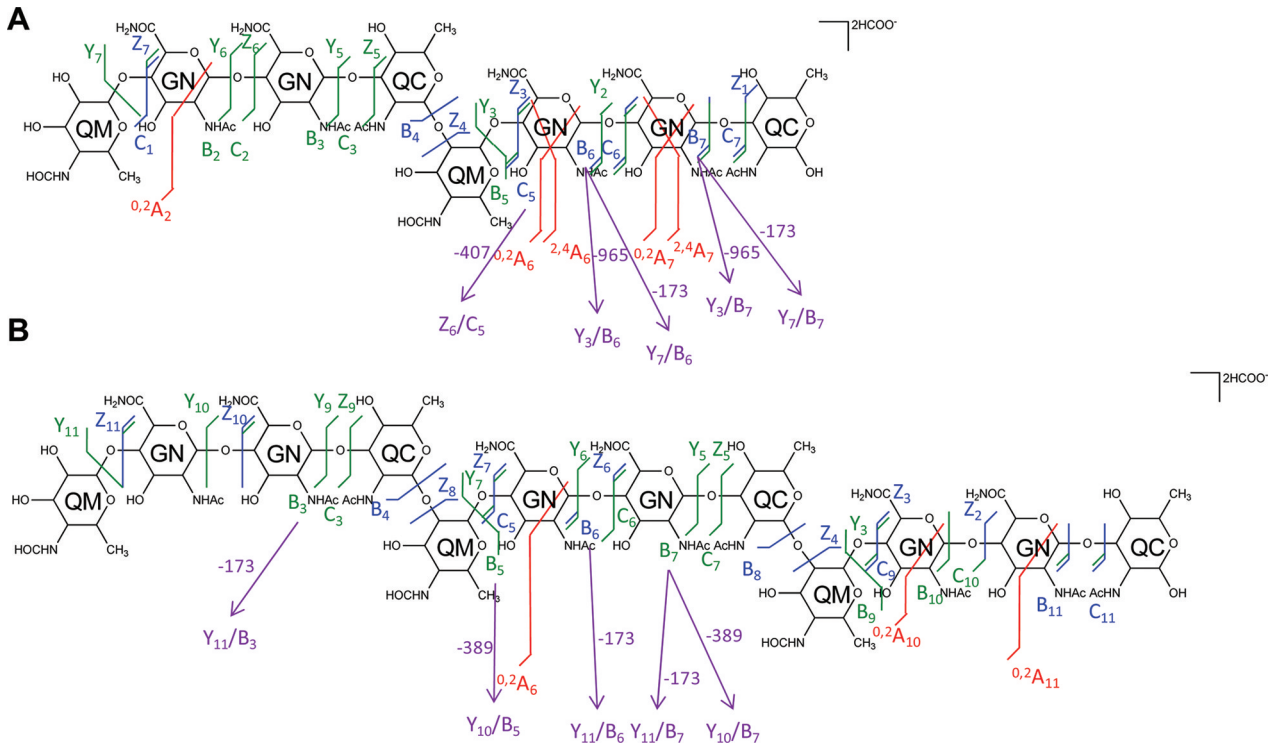

Figure 6. Similar fragment ions are observed for saccharides in negative ion mode. CID MS^2 fragmentations of the $[M + 2HCOO]^{2-}$ ion of saccharide chains [4,2,2][0,0,0] at m/z 846.3049 (A) and [6,3,3][0,0,0] at m/z 1242.4535 (B) were obtained in negative ion mode using a Solarix FT-ICR mass spectrometer and are displayed on the chemical structures. Monosaccharide residue abbreviations QM (Qui4NFm), GN (GalNAcAN), and QC (QuiNAc) are shown inside the six-member rings for the sake of clarity.

of [4,2,2][0,0,0], singly charged product ions at m/z 646.2155 and 660.2312, corresponding to the compositions [2,0,1]-[0,0,0] and [2,1,0][0,0,0], respectively, were observed in the MS^3 spectrum of [6,3,3][0,0,0], suggesting the Qui4NFm-GalNAcAN-GalNAcAN-QuiNAc sequence. The presence of the ions at m/z 444.1574 and 473.1473, corresponding to the compositions [1,1,0][0,0,0] and [2,0,0][0,0,0], respectively, also confirmed the monosaccharide sequence. The base peak in the MS^2 spectrum, m/z 1126.9037, corresponding to the doubly charged [6,2,3][0,0,0] species, implies the position of a QuiNAc residue at either the nonreducing end or the reducing end of the sequence. In the tandem MS spectrum of the [M +

dx.doi.org/10.1021/bi201450v | *Biochemistry* 2011, 50, 10941–10950

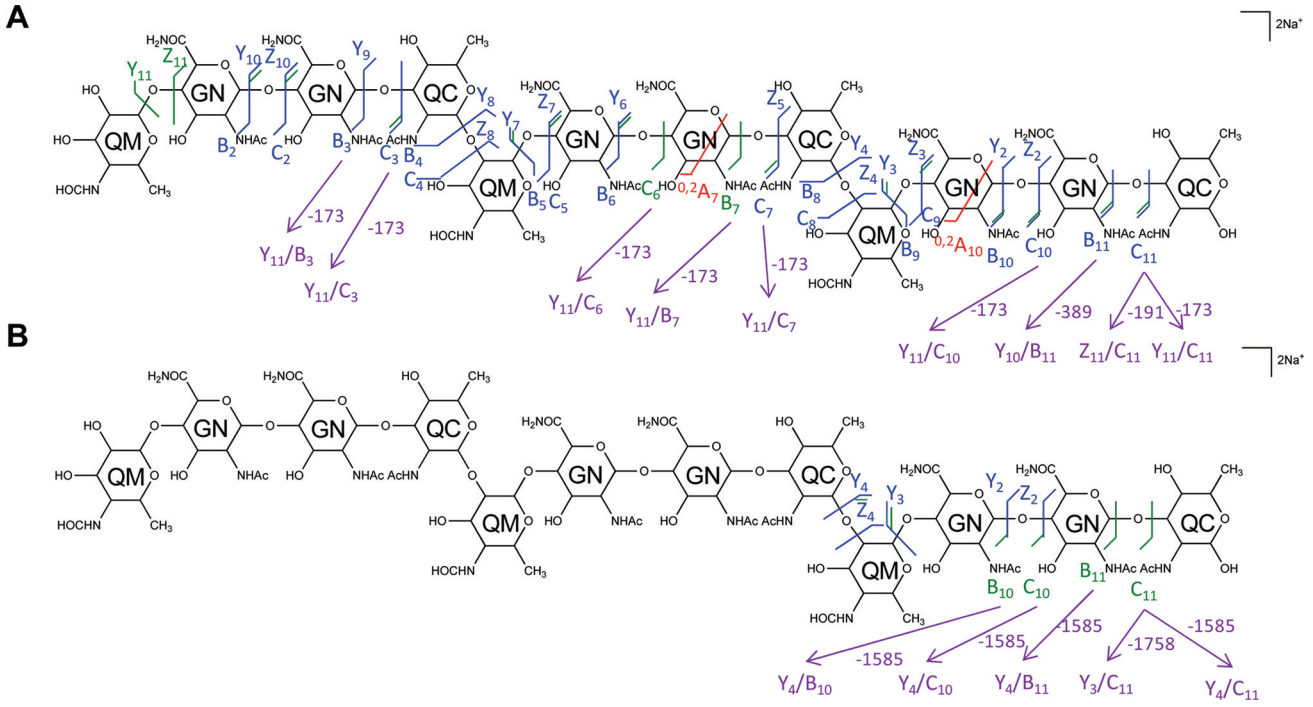

Figure 7. Multistage tandem MS reveals the structural linkage for [6,3,3][0,0,0]. Tandem MS of saccharide [6,3,3][0,0,0], $[M + 2Na]^{2+}$ ion at m/z 1220.4479, was performed on an LTQ-Oribtrap XL mass spectrometer in positive ion mode. CID fragmentations of the precursor ion at m/z 1220.4479 (A) and MS^3 of the product ion at m/z 833.3003 (B) are displayed on the chemical structures. Monosaccharide residue abbreviations QM (Qui4NFm), GN (GalNAcAN), and QC (QuiNAc) are shown inside the six-member rings for the sake of clarity. All fragments contain Na.

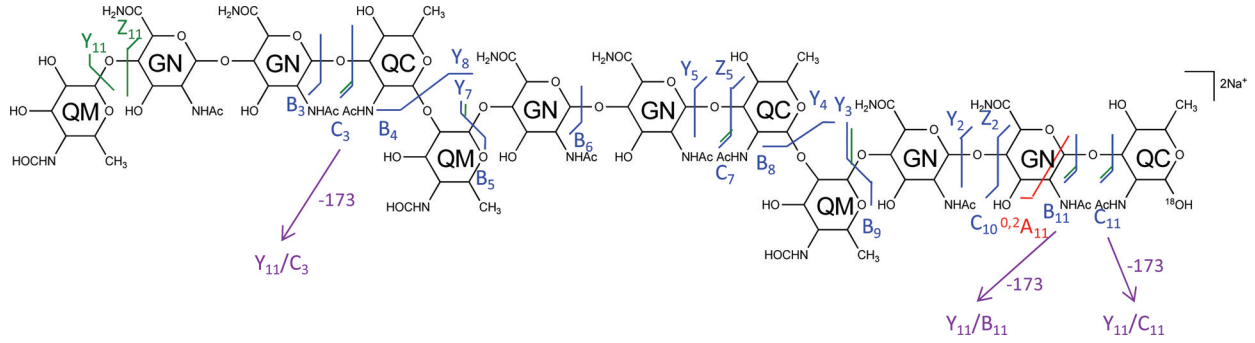

Figure 8. Tandem MS of ^{18}O-labeled saccharide [6,3,3][0,0,0] reveals the reducing end residue. Tandem MS of ^{18}O-labeled saccharide [6,3,3][0,0,0], $[M + 2Na]^{2+}$ ion at m/z 1221.4487, was performed on an LTQ-Oribtrap XL mass spectrometer in positive ion mode. CID fragmentations of the precursor ion are indicated on the chemical structure. Monosaccharide residue abbreviations QM (Qui4NFm), GN (GalNAcAN), and QC (QuiNAc) are shown inside the six-member rings for the sake of clarity. All fragments contain Na.

$2Na]^{2+}$ ion of ^{18}O-labeled [6,3,3][0,0,0] (Figure 5 and Table 5 of the Supporting Information), the base peak was observed at m/z 1126.9044, corresponding to [6,2,3][0,0,0]. This result indicates that a QuiNAc residue is located at the reducing end of the linear oligosaccharide chain. As was observed in the MS^2 spectrum of ^{18}O-labeled [4,2,2][0,0,0], the appearance of the signals at m/z 662.2365 and 646.2166, which correspond to [2,1,0][0,0,0] with one ^{18}O atom replacing one ^{16}O atom and [2,0,1][0,0,0], respectively, supports the conclusion that a QuiNAc residue serves as the reducing end of this oligosaccharide. Therefore, [6,3,3][0,0,0] is composed of three tetrasaccharide repeats, Qui4NFm-GalNAcAN-GalNAcAN-QuiNAc, in series, with a Qui4NFm residue at the nonreducing end and a QuiNAc residue at the reducing end (Figure 3B).

The multistage tandem MS fragments of native and ^{18}O-labeled [6,3,3][0,0,0] are displayed on their chemical structures in Figures 7 and 8. A few cross-ring cleavages were observed on the GalNAcAN residues in the MS^2 spectrum of [6,3,3][0,0,0], and no linkage information can be deduced from them.

Tandem MS of native [6,3,3][0,0,0] was also conducted in negative ion mode using an FT-ICR mass spectrometer (Figure 3B of the Supporting Information). The detailed interpretations of the tandem MS result are presented in Figure 6B and Table 3 of the Supporting Information. From the observed products that arose via glycosidic bond cleavages, [6,3,3][0,0,0] is confirmed to be composed of three tetrasaccharide repeats, Qui4NFm-GalNAcAN-GalNAcAN-QuiNAc, in series. The cross-ring cleavages observed in tandem mass spectra acquired in the negative ion mode did not allow unambiguous assignment of linkages.

dx.doi.org/10.1021/bi201450v | *Biochemistry* 2011, 50, 10941–10950

Table 2. High-Resolution and High-Mass Accuracy MS Is Necessary for Interpretation of Saccharide Composition[a]

observed peak (m/z)	charge	interpretation 1	mass error for assignment 1 (ppm)	interpretation 2	mass error for assignment 2 (ppm)
846.3090	2	[2,0,1][1,4,1]	32.4	[4,2,2][0,0,0]	3.5
1242.4604	2	[4,1,2][1,4,1]	22.2	[6,3,3][0,0,0]	2.5
1107.4107	3	[6,2,3][1,4,1]	19.8	[8,4,4][0,0,0]	5.1
1371.5132	3	[8,3,4][1,4,1]	17.2	[10,5,5][0,0,0]	5.3

[a]The mass errors from two different potential assignments for the observed monoisotopic masses for saccharides composed of two to five tetrasaccharide repeats are listed. Saccharide compositions are given as [GalNAcAN,QuiNAc,Qui4NFm][HexNAc,Hex,Kdo].

DISCUSSION

OAg-containing saccharides obtained after hydrolysis of the components in preparations of Ft LPS have been assumed to consist of OAg chains attached to the $HexNAcHex_4Kdo$ core.[17] In this work, OAg saccharides attached to the $HexNAcHex_3Kdo$ core, the $HexNAcHex_4Kdo$ core, and OAg saccharides without an attached core were identified in hydrolysates of LPS preparations from both the LVS and SchuS4 strains. It is likely that the published studies using NMR failed to detect the coreless saccharides. In this study and in previous work,[18] coreless saccharides were not detected in the permethylated samples, possibly because of their poor solubility in organic solvents during the derivatization procedure. Similarly, previous studies may not have detected OAg core saccharides containing the $HexNAcHex_3Kdo$ core because of the higher abundance of OAg-$HexNAcHex_4Kdo$ saccharides in both LVS and SchuS4.

It was necessary to use high-resolution and high-mass accuracy MS to reach a definitive interpretation of the compositions of saccharides derived from Ft LPS preparations. For example, the monoisotopic peak at m/z 846.3090 (2+) could have been interpreted as [2,0,1][1,4,1] with an ~30 ppm mass error that is within the tolerable range for low-resolution mass spectrometers (Table 2). By contrast, the assignment of the same peak as [4,2,2][0,0,0] results in a mass error of 3.5 ppm, which is within the mass error tolerance for the high-resolution and high-accuracy mass spectrometers used in this study. Thus, the application of high-resolution and high-accuracy MS allowed the identification of previously unidentified coreless saccharides[17,18] in fractions released from Ft LPS preparations.

CID was used to achieve fragmentation of the coreless saccharides with two and three tetrasaccharide repeats in this study. Extensive glycosidic bond cleavages were observed in both positive and negative ionization mode tandem MS experiments. The information allowed a consistent interpretation regarding the monosaccharide sequences of the saccharides. Other fragmentation techniques, such as electron transfer dissociation (ETD)[28] and electron capture dissociation (ECD),[29] which generate mainly cross-ring cleavages for carbohydrates,[30,31] and/or other chemical derivatization of the native saccharides, such as peracetylation, might be helpful in providing additional detail concerning the glycosidic linkage positions in these coreless saccharides.

Although mass spectrometry has the advantage of accurately detecting minor components compared to other detection methods such as NMR, it is not sufficient to distinguish isomers of the monosaccharide residues because it only provides m/z values of the analytes. It is insufficient to determine the identity of the monosaccharide residues, and other complementary detection techniques, for example, NMR and glycosyl composition, are needed to identify the actual monosaccharide residues.

Ft OAg had been reported by Vinogradov and co-workers, on the basis of NMR analysis,[16,17] or Prior et al., on the basis of MS analysis,[18] to have repeats of the structure →4)-GalNAcAN-(α1→4)-GalNAcAN-(α1→3)-QuiNAc-(β1→2)-Qui4NFm-(β1→ or to be composed of $(GalNAcAN)_2QuiNAcQui4NFm$, respectively. Both groups proposed that the QuiNAc residue is attached to the core based on similarities in the sugar composition of the OAg repeat unit of Ft compared to other Gram-negative bacteria[16,17] and the deduced putative functions of the proteins encoded in the OAg biosynthetic gene cluster of Ft.[18] This study confirmed the previously reported Ft OAg repeat structure and showed that QuiNAc is the reducing end residue and that a Qui4NFm is the residue at the nonreducing end of coreless OAg saccharides.

This high-resolution and high-mass accuracy tandem MS study demonstrated that the coreless saccharides have the Qui4NFm-GalNAcAN-GalNAcAN-QuiNAc monosaccharide sequence attached in series. This is the same as the recently reported Ft CPS tetrasaccharide repeat sequence.[20] The saccharides observed in this study may derive from LPS chains in the process of synthesis, before or during transfer from the carrier oligosaccharide to core lipid A in the Ft inner membrane, a process documented for other Gram-negative bacteria.[32−34] The considerably higher abundance of coreless saccharides in the SchuS4 strain versus the LVS strain observed in this study is consistent with the presence of thicker capsules in virulent Ft strains compared with LVS.[35] Differences in abundances of saccharides may also arise from the culture conditions of the bacteria used for the commercial LVS versus that for the in-house SchuS4 LPS preparations.[26] Other methods of separating LPS and CPS[36,20] might be helpful in revealing the biological role of the coreless OAg saccharides observed in this study..

This study identified three structurally distinct types of OAg-containing saccharides present in hydrolysates of Ft LPS preparations: those with a $HexNAcHex_4Kdo$ core, those with a $HexNAcHex_3Kdo$ core, and those with no core. Each of these has the potential to present unique epitopes for antibody reactivity. Preparative chromatographic separation of homogeneous OAg-containing and core saccharides is therefore necessary to map epitopes targeted by protective anti-Ft LPS antibodies toward development of vaccines and immunotherapeutics for tularemia.

ASSOCIATED CONTENT

Supporting Information

Supplemental tables and figures. This material is available free of charge via the Internet at http://pubs.acs.org.

AUTHOR INFORMATION

Corresponding Author

*Department of Biochemistry, Boston University School of Medicine, MS Resource, 670 Albany St., Boston, MA 02118.

Telephone: (617) 638-6762. Fax: (617) 638-6760. E-mail: jzaia@bu.edu.

Funding

This research is supported by National Institutes of Health (NIH) Contract HHSN272200900054C and NIH Grants P41 RR010888, S10 RR015942, S10 RR020946, and S10 RR025082.

■ ACKNOWLEDGMENTS

We thank Mathew Walsh for preliminary results, Yu Huang for help with data analysis, and Xiang Yu and Liang Han for technical help in oligosaccharide derivatization.

■ ABBREVIATIONS

Ft, *Francisella tularensis*; LPS, lipopolysaccharide; OAg, *O*-antigen; LVS, live vaccine strain; CPS, capsular polysaccharide; Qui4NFm, 4,6-dideoxy-4-formamido-D-glucose; QuiNAc, 2-acetamido-2,6-dideoxy-*O*-D-glucose; GalNAcAN, 2-acetamido-2-deoxy-*O*-D-galacturonamide; Hex, hexose; HexNAc, *N*-acetylhexosamine; Kdo, 3-deoxy-D-*manno*-oct-2-ulosonic acid; NMR, nuclear magnetic resonance; MS, mass spectrometry; LC, liquid chromatography; MS^n, tandem mass spectrometry; SEC, size exclusion chromatography; MALDI-TOF, matrix-assisted laser desorption ionization time-of-flight; DHB, 2,5-dihydroxybenzoic acid; TFA, trifluoroacetic acid; HILIC, hydrophilic interaction chromatography; MUF, makeup flow; CID, collision-induced dissociation; FT-ICR, Fourier transform ion cyclotron resonance; ETD, electron transfer dissociation; ECD, electron capture dissociation.

■ REFERENCES

(1) Saslaw, S., Eigelsbach, H. T., Prior, J. A., Wilson, H. E., and Carhart, S. (1961) Tularemia vaccine study. II. Respiratory challenge. *Arch. Intern. Med. 107*, 702−714.

(2) Keim, P., Johansson, A., and Wagner, D. M. (2007) Molecular epidemiology, evolution, and ecology of *Francisella*. *Ann. N.Y. Acad. Sci. 1105*, 30−66.

(3) Sjostedt, A. (2007) Tularemia: History, epidemiology, pathogen physiology, and clinical manifestations. *Ann. N.Y. Acad. Sci. 1105*, 1−29.

(4) Tarnvik, A., and Chu, M. C. (2007) New approaches to diagnosis and therapy of tularemia. *Ann. N.Y. Acad. Sci. 1105*, 378−404.

(5) Dennis, D. T., Inglesby, T. V., Henderson, D. A., Bartlett, J. G., Ascher, M. S., Eitzen, E., Fine, A. D., Friedlander, A. M., Hauer, J., Layton, M., Lillibridge, S. R., McDade, J. E., Osterholm, M. T., O'Toole, T., Parker, G., Perl, T. M., Russell, P. K., and Tonat, K. (2001) Tularemia as a biological weapon: Medical and public health management. *JAMA, J. Am. Med. Assoc. 285*, 2763−2773.

(6) Eigelsbach, H. T., and Downs, C. M. (1961) Prophylactic effectiveness of live and killed tularemia vaccines. I. Production of vaccine and evaluation in the white mouse and guinea pig. *J. Immunol. 87*, 415−425.

(7) Burke, D. S. (1977) Immunization against tularemia: Analysis of the effectiveness of live *Francisella tularensis* vaccine in prevention of laboratory-acquired tularemia. *J. Infect. Dis. 135*, 55−60.

(8) Sandstrom, G. (1994) The tularaemia vaccine. *J. Chem. Technol. Biotechnol. 59*, 315−320.

(9) Conlan, J. W. (2011) Tularemia vaccines: Recent developments and remaining hurdles. *Future Microbiol. 6*, 391−405.

(10) Oyston, P. C. (2009) *Francisella tularensis* vaccines. *Vaccine 27* (Suppl. 4), D48−D51.

(11) Fulop, M. J., Webber, T., Manchee, R. J., and Kelly, D. C. (1991) Production and characterization of monoclonal antibodies directed against the lipopolysaccharide of *Francisella tularensis*. *J. Clin. Microbiol. 29*, 1407−1412.

(12) Fulop, M., Mastroeni, P., Green, M., and Titball, R. W. (2001) Role of antibody to lipopolysaccharide in protection against low- and high-virulence strains of *Francisella tularensis*. *Vaccine 19*, 4465−4472.

(13) Lu, Z., Roche, M. I., Hui, J. H., Unal, B., Felgner, P. L., Gulati, S., Madico, G., and Sharon, J. (2007) Generation and characterization of hybridoma antibodies for immunotherapy of tularemia. *Immunol. Lett. 112*, 92−103.

(14) Roche, M. I., Lu, Z., Hui, J. H., and Sharon, J. (2011) Characterization of monoclonal antibodies to terminal and internal *O*-antigen epitopes of *Francisella tularensis* lipopolysaccharide. *Hybridoma Hybridomics 30*, 19−28.

(15) Gunn, J. S., and Ernst, R. K. (2007) The structure and function of *Francisella* lipopolysaccharide. *Ann. N.Y. Acad. Sci. 1105*, 202−218.

(16) Vinogradov, E. V., Shashkov, A. S., Knirel, Y. A., Kochetkov, N. K., Tochtamysheva, N. V., Averin, S. F., Goncharova, O. V., and Khlebnikov, V. S. (1991) Structure of the O-antigen of *Francisella tularensis* strain 15. *Carbohydr. Res. 214*, 289−297.

(17) Vinogradov, E., Perry, M. B., and Conlan, J. W. (2002) Structural analysis of *Francisella tularensis* lipopolysaccharide. *Eur. J. Biochem. 269*, 6112−6118.

(18) Prior, J. L., Prior, R. G., Hitchen, P. G., Diaper, H., Griffin, K. F., Morris, H. R., Dell, A., and Titball, R. W. (2003) Characterization of the O antigen gene cluster and structural analysis of the O antigen of *Francisella tularensis* subsp. *tularensis*. *J. Med. Microbiol. 52*, 845−851.

(19) Thirumalapura, N. R., Goad, D. W., Mort, A., Morton, R. J., Clarke, J., and Malayer, J. (2005) Structural analysis of the *O*-antigen of *Francisella tularensis* subspecies *tularensis* strain OSU 10. *J. Med. Microbiol. 54*, 693−695.

(20) Apicella, M. A., Post, D. M., Fowler, A. C., Jones, B. D., Rasmussen, J. A., Hunt, J. R., Imagawa, S., Choudhury, B., Inzana, T. J., Maier, T. M., Frank, D. W., Zahrt, T. C., Chaloner, K., Jennings, M. P., McLendon, M. K., and Gibson, B. W. (2010) Identification, characterization and immunogenicity of an O-antigen capsular polysaccharide of *Francisella tularensis*. *PLoS One 5*, e11060.

(21) Westphal, O., and Jann, K. (1965) Bacterial Lipopolysaccharides Extraction with Phenol-Water and Further Applications of the Procedure. *Methods Carbohydr. Chem. 5*, 83−91.

(22) Apicella, M. A., Griffiss, J. M., and Schneider, H. (1994) Isolation and characterization of lipopolysaccharides, lipooligosaccharides, and lipid A. *Methods Enzymol. 235*, 242−252.

(23) Ciucanu, I., and Kerek, F. (1984) A simple and rapid method for the permethylation of carbohydrates. *Carbohydr. Res. 131*, 209−217.

(24) Ciucanu, I., and Costello, C. E. (2003) Elimination of oxidative degradation during the per-O-methylation of carbohydrates. *J. Am. Chem. Soc. 125*, 16213−16219.

(25) Staples, G. O., Naimy, H., Yin, H., Kileen, K., Kraiczek, K., Costello, C. E., and Zaia, J. (2010) Improved hydrophilic interaction chromatography LC/MS of heparinoids using a chip with postcolumn makeup flow. *Anal. Chem. 82*, 516−522.

(26) Cherwonogrodzky, J. W., Knodel, M. H., and Spence, M. R. (1994) Increased encapsulation and virulence of *Francisella tularensis* live vaccine strain (LVS) by subculturing on synthetic medium. *Vaccine 12*, 773−775.

(27) Domon, B., and Costello, C. E. (1988) A systematic nomenclature for carbohydrate fragmentations in FAB-MS/MS spectra of glycoconjugates. *Glycoconjugate J. 5*, 397−409.

(28) Syka, J. E., Coon, J. J., Schroeder, M. J., Shabanowitz, J., and Hunt, D. F. (2004) Peptide and protein sequence analysis by electron transfer dissociation mass spectrometry. *Proc. Natl. Acad. Sci. U.S.A. 101*, 9528−9533.

(29) Zubarev, R. A., Kelleher, N. L., and McLafferty, F. W. (1998) Electron capture dissociation of multiply charged protein cations. A nonergodic process. *J. Am. Chem. Soc. 120*, 3265−3266.

(30) Han, L., and Costello, C. E. (2011) Electron transfer dissociation of milk oligosaccharides. *J. Am. Soc. Mass Spectrom. 22*, 997−1013.

(31) Adamson, J. T., and Hakansson, K. (2007) Electron capture dissociation of oligosaccharides ionized with alkali, alkaline earth, and transition metals. *Anal. Chem. 79*, 2901−2910.

(32) Lengeler, J., Drews, G., and Schlegel, H. (2009) Assembly of cellular surface structures. In *Biology of the Prokaryotes*, pp 555−570, Blackwell Science Ltd., Oxford, U.K.
(33) Metzler, D. (2003) Biosynthesis of bacterial cell walls. In *Biochemistry: The chemical reactions of living cells*, pp 1160−1169, Academic Press, New York.
(34) Zhao, J., and Raetz, C. R. (2010) A two-component Kdo hydrolase in the inner membrane of *Francisella novicida*. *Mol. Microbiol. 78*, 820−836.
(35) Hood, A. M. (1977) Virulence factors of *Francisella tularensis*. *J. Hyg. 79*, 47−60.
(36) Adam, O., Vercellone, A., Paul, F., Monsan, P. F., and Puzo, G. (1995) A nondegradative route for the removal of endotoxin from exopolysaccharides. *Anal. Biochem. 225*, 321−327.